

# Numerical Simulation of Interaction between an L1 Stream and an Accretion Disk in a Close Binary System.

Hidekazu FUJIWARA, Makoto MAKITA, Takizo NAGAE and Takuya MATSUDA

*Department of Earth and Planetary Sciences, Kobe University, Kobe 657-8501*

(Received )

The hydrodynamic behavior of an accretion disk in a close binary system is numerically simulated. Calculation is made for a region including the compact star and the gas-supplying companion. The equation of state is that of an ideal gas characterized by the specific heat ratio  $\gamma$ . Two cases with  $\gamma$  of 1.01 and 1.2 are studied. Our calculations show that the gas, flowing from the companion via a Lagrangian L1 point towards the accretion disk, forms a fine gas beam (L1 stream), which penetrates into the disk. No hot spot therefore forms in these calculations. Another fact discovered is that the gas rotating with the disk forms, on collision with the L1 stream, a bow shock wave, which may be called an L1 shock. The disk becomes hot because the L1 shock heats the disk gas in the outer parts of the disk, so that the spiral shocks wind loosely even with  $\gamma = 1.01$ . The L1 shock enhances the non-axisymmetry of the density distribution in the disk, and therefore the angular momentum transfer by the tidal torque works more effectively. The maximum of the effective  $\alpha$  becomes  $\sim 0.3$ . The 'hot spot' is not formed in our simulations, but our results suggest the formation of the 'hot line', which is the L1 shock elongated along the penetrating L1 stream.

## §1. Introduction and Summary

### 1.1. *Discovery of Spiral Structure*

In recent years, Steeghs, Harlaftis & Horne<sup>1)</sup> discovered, with use of the Doppler tomography technique, a spiral structure in the accretion disk of the dwarf nova IP Pegasi, occurring in its outburst phase. After the discovery of Steeghs et al.,<sup>1)</sup> similar spiral structures have been found on many other accretion disks.<sup>2-4)</sup> Such spiral structures are generally thought to be unobservable during quiescent phases of dwarf novae, but Neustroev & Borisov<sup>5)</sup> observed them in a quiescent phase in U Gem.

Formation of spiral-shape shocks in an accretion disk of a close binary had been predicted based on two-dimensional numerical simulations, by Sawada, Matsuda & Hachisu,<sup>6,7)</sup> and Sawada et al.<sup>8)</sup> Similar two-dimensional numerical simulations performed by many researchers thereafter all confirmed the presence of the spiral shock waves.<sup>9)</sup> Self-similar solutions of the spiral shocks were also obtained.<sup>15)</sup> Angular momentum loss at the spiral shocks provides a different mechanism from the conventional  $\alpha$ -viscosity one.

Three-dimensional simulations have also been made on the same object, but given no results completely agreeing with one another. Most of the three-dimensional numerical simulations of accretion disks so far performed used the particle methods such as the SPH method,<sup>16)</sup> and mostly failed in finding any spiral shock.

On the other hand, Yukawa, Matsuda & Boffin<sup>24)</sup> observed, with use of the SPH method, spiral shocks on the assumption that the specific heat ratio  $\gamma$  was 1.2. Lanzafame & Belvedere,<sup>25,26)</sup> Boffin, Haraguchi & Matsuda<sup>27)</sup> also observed spiral shocks in their recent SPH calculations. This disagreement is considered to be due to the difference in resolution, more concretely, in the number of particles. That is, use of a

sufficient number of particles, which enhances the resolution, leads to the observation of spiral shocks.

With the finite difference/volume method, having a high accuracy compared to the SPH method, it is expected that a detailed structure of an accretion disk be readily observed. Sawada & Matsuda<sup>28)</sup> performed simulation by means of the three-dimensional finite volume method for the first time. Although the result shows the presence of spiral shocks, no definite statement was made with respect to this phenomenon, since the calculation time adopted by them was as short as half an orbital period.

In recent years, our group conducted a series of the three-dimensional finite volume calculations and confirmed the presence of spiral shocks in all cases.<sup>29-31)</sup> These calculations, however, restricted the calculation region to the vicinity of the compact star and did not include the companion. The gas was assumed to flow into through a rectangular hole located at the Lagrangian L1 point. Since most of the calculation region was filled with a low-pressure gas, the gas flowing into the region from the hole underwent a rapid expansion, thereby forming what is known as under-expanded jet. The flow (L1 stream) thus formed appeared to interact with the accretion disk in a complex manner. The hole, being artificial, made the L1 stream an under-expanded jet having a square cross section, which was unnatural. It has therefore been desired that simulation be made with the calculation region extending up to the companion, whereby the true shape of the L1 stream could be observed.

Bisikalo et al.<sup>32)</sup>rf:36 also made very similar works to the present work, and the relation between our results and theirs will be discussed in the last section.

## 1.2. *Difference between 2D and 3D Results*

Although radiative cooling has an important effect on the behavior of an accretion disk, it is however very difficult to incorporate the effect accurately in three-dimensional calculations. To avoid this difficulty, we use as the equation of state of the gas the one for an ideal gas and, as the specific heat ratio of the gas  $\gamma$ , a value smaller than 5/3, thereby simulating the effect of radiative cooling to some extent.

What has puzzled us most in interpreting the results obtained by our three-dimensional calculations is that they greatly differ from those obtained by two-dimensional calculations (see figure 1). With the two-dimensional calculations, we can obtain a clear correlation between  $\gamma$  and the degree of winding-in of spiral shocks: smaller pitch angle and tighter winding angle with smaller  $\gamma$  (Makita et al.<sup>31)</sup>, Matsuda et al.<sup>37)</sup>). A smaller  $\gamma$  corresponds, with the gas undergoing an adiabatic change, a smaller temperature elevation. The limit of  $\gamma = 1$  corresponds to an isothermal change. In the presence of shocks this is not necessarily so, but with two-dimensional calculations, a small  $\gamma$  generally means a low temperature of the accretion disk, which corresponds to a low sound speed and thus to a large Mach number. It is natural that in this case the spiral shocks wind in tightly.

On the other hand, as is clear from figure 1, with three-dimensional calculations, the obtained spiral shocks seem to wind in very mildly, in particular when  $\gamma = 1.01$ .

This finding has long been a mystery to us. Two possible explanations may be given for this difference: numerical and physical ones. Numerical explanations are:

1. The calculation region does not contain the companion, so that the L1 stream does not have a natural shape. This fact may affect the structure of the accretion

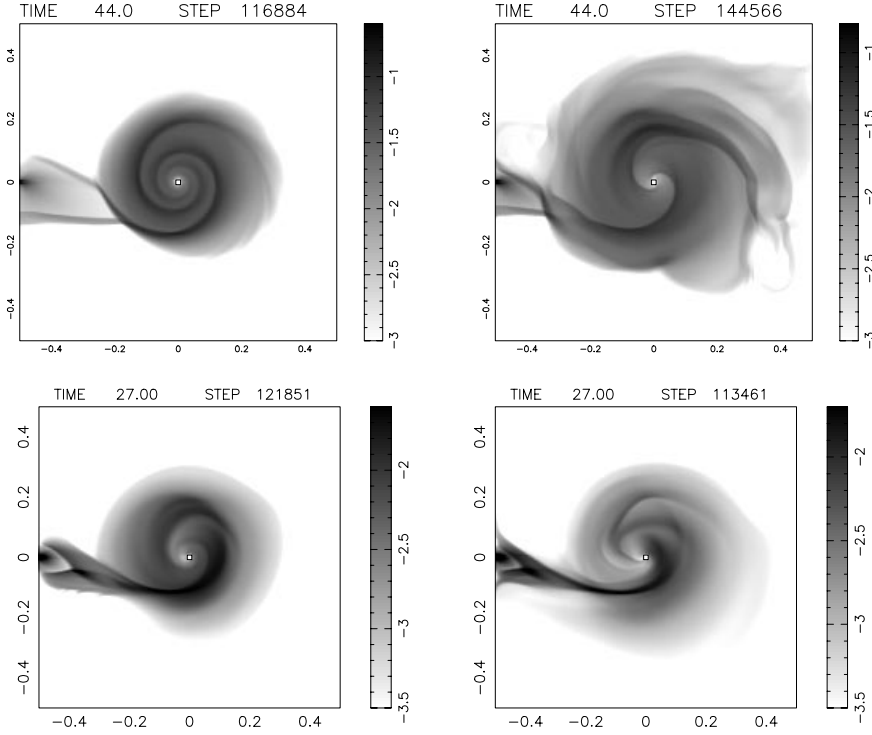


Fig. 1. Difference between the 2D and 3D results: The density distributions obtained by 2D calculation (top) and those by 3D calculation on the rotational plane (bottom), with the specific heat ratio  $\gamma$  being 1.01 (left) and 1.2 (right). The calculation region is restricted to the vicinity of the compact star and exclude the companion. With 2D calculations smaller  $\gamma$  leads to tighter winding. On the other hand, 3D calculations do not show such an effect clearly. The strange shape of the L1 stream is due to the fact that the L1 stream comes from a square hole placed at the L1 point and, as a result, forms an under-expanded jet. (After Makita et al.<sup>31)</sup>)

disk.

2. In early stages of the calculation, a high-temperature gas is assumed to be present over the entire calculation region. This assumption is necessary for the calculation to proceed stably. In two-dimensional calculations, an accretion disk forms with elapse of time, while the gas initially placed is removed from the region of the accretion disk and has no influence on the result.
3. With three-dimensional calculations, however, the high-temperature gas remains above the accretion disk and may mix with the disk gas, thereby increasing the disk temperature. This effect may be significant at the central part of the disk where it is thin.

In order to solve these problems, the present study enlarges the calculation region to an extent covering the companion. Besides, in order to check the influence of the high-temperature gas initially placed, the temperature and density of the gas are intentionally decreased. As a result it has been found that the above numerical factors are not crucial in causing the difference between the calculation results. It is then concluded that the difference in the results between two-dimensional and three-dimensional

calculations should be explained on physical basis rather than numerical basis.

The results of the present calculations taking the companion into account, to be shown later, indicate that the basic features of the accretion disk does not differ very much from that obtained by calculations without the companion.

### 1.3. *Penetration of the L1 Stream into the Disk and the Loss of the Angular Momentum of the Disk Due to the Penetration*

Our calculations covering a region including the companion has revealed that the L1 stream, on collision with the disk, penetrates into the disk like a spear and does not decrease its velocity by forming a hot spot. We refer to this phenomenon as “penetration” hereinafter. The presence of the penetration was not convincingly confirmed in the previous three-dimensional calculations due to the L1 stream having an unnatural shape. However, here, thanks to a visualization technique adopted by us, the L1 stream reveals its detailed structure. Note that *with two-dimensional calculations the penetration can never occur*, which is understandable from geometrical consideration. This is an essential difference between three-dimensional and two-dimensional calculations.

The disk gas supersonically rotating around the compact star must form, on collision with the high-density, low-temperature L1 stream resembling a spear, a bow shock, which we call L1 shock. The bow shock thus formed may be viewed as a hot line or a heated wall rather than a hot spot. At the L1 shock the disk gas gives the penetrating L1 stream its angular momentum. The gas is at last released into the inner parts of the disk and mixes with the disk gas. The angular momentum, which is transferred from the disk gas to the penetrating L1 stream at the L1 shock, is therefore finally redistributed into the disk, if tidal torque from the secondary star dose not work. But, the L1 shock and the penetrating L1 stream enhance the non-axisymmetry in density distribution produced by spiral shocks in the disk and, as a result, tidal torque from the secondary star transfers more effectively the angular momentum of the disk to the angular momentum of the orbital rotation of the binary system. The disk gas therefore loses angular momentum and accretes onto the primary star. In figure 2 schematic presentation of the spiral shocks, the L1 stream and the L1 shock are shown.

Here we present an analogy between a gas centrifuge to enrich uranium and the accretion disk with the L1 stream. In order to enrich uranium, there have been available ultra gas centrifuges, which comprise a cylinder rotating at a high speed and containing uranium hexa-fluoride. The cylinder is equipped in the inside thereof a stationary tube named “scoop” for recovering enriched or depleted products of the uranium compound. The rotating gas forms a bow shock on collision with the scoop, and loses its angular momentum, whereby a meridional flow called counter current is formed (Matsuda, Tamura & Sawada<sup>38</sup>). The scoop works as a sink of angular momentum, because the scoop and gas centrifuge are fixed to ground. The L1 stream in the present case however dose not work as a sink of angular momentum itself. The role of the L1 stream is only to get angular momentum from the disk gas, and the secondary star actually plays the role of a sink of angular momentum.

When calculation is made by means of a three-dimensional simulation, the angular momentum of the disk gas is lost on collision with the L1 stream and, at the same time, the entropy and temperature of the disk gas increase. As a result, the sound speed increases and the Mach number in the disk is reduced compared to that with

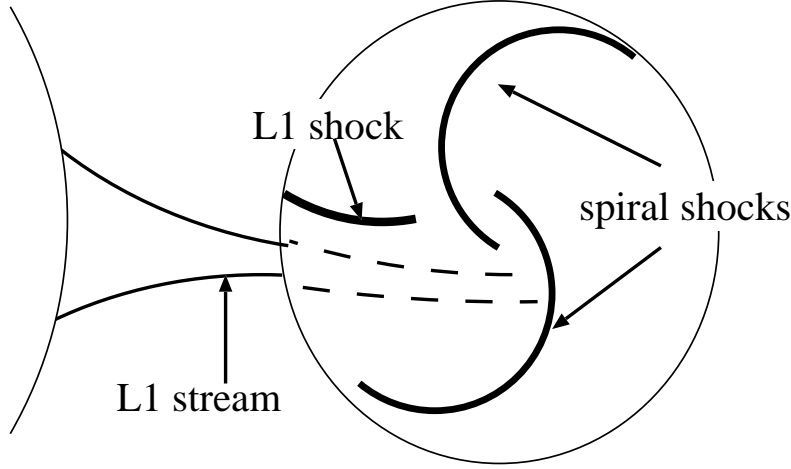


Fig. 2. Schematic presentation of the flows in the accretion disk, showing: the companion star (left end), the accretion disk (a large circle), the spiral shocks, the L1 stream flowing from the companion to the accretion disk through L1 point and the L1 shock, on which rotating disk gas collides with the L1 stream and deflects its direction.

two-dimensional calculations, so that the spiral shocks wind in mildly.

Section 2 briefly describes the method of calculation. Section 3 discusses the effect of the numerical assumptions on the results. Section 4 discusses the detailed structure of the accretion disk and the L1 stream. We compare the three-dimensional calculations and two-dimensional ones in detail and shows that the difference can be explained on a physical basis rather than on a numerical one. Section 5 gives a summary and discussion.

## §2. Numerical Models

### 2.1. Method of Numerical Simulation and Basic Assumptions

We use, as before, the Simplified Flux Vector Splitting (SFS) finite volume method proposed by Jyounouchi et al.,<sup>39)</sup> Shima & Jyounouchi.<sup>40)</sup> This method, being a variation of AUSM type methods, has the feature of being simple and stable. As to the detail of the numerical scheme and the SFS scheme see Makita et al.<sup>31)</sup> We use a MUSCL-type technique, thereby keeping the spatial and temporal accuracy at second order levels. We consider the gas as a perfect gas and do not take into account such complex effects as viscosity, radiation and magnetic field. The equation of state is as follows.

$$p = (\gamma - 1) \left[ e - \frac{1}{2} \rho (u^2 + v^2 + w^2) \right], \quad (2.1)$$

where  $p, \rho, e$  are the pressure, density and total energy per unit volume of the gas, respectively, and  $\gamma$  is the specific heat ratio;  $u, v, w$  are the velocity component in the directions of  $x, y, z$ , respectively. We use as the specific heat ratio, not the value of

5/3, which is that of an adiabatic gas, but smaller values and mainly  $\gamma = 1.01, 1.2$ . In the absence of shocks, the entropy would be kept constant and the temperature would change as  $T \propto \rho^{\gamma-1}$ . The temperature change thus becomes nearly isothermal at a limit of  $\gamma$  approaching 1. Our calculations, however, produce shocks, where the entropy of the gas increases. Accordingly,  $\gamma \sim 1$  does not necessarily mean that the accretion disk is nearly isothermal.

Indeed, with use of the same value for  $\gamma$ , the temperature and the entropy of an accretion disk obtained by means of three-dimensional calculations differ from those by two-dimensional ones significantly. This is attributable to whether or not shocks are present and to the difference in the strengths of the shocks. By selection of  $\gamma = 1.01$ , we intend to increase the cooling effect as much as possible while keeping numerical accuracy. The larger  $\gamma = 1.2$  is selected because a  $\gamma$  larger than this would not produce an accretion disk itself. We thus study the two extreme cases.

We consider, as the model of a binary, a system consisting of a compact star (primary star) with mass  $M_1$  and a mass-losing companion with mass  $M_2$ . The mass ratio  $q = M_2/M_1$  is fixed at 1 in the present study, while with IP Peg  $q \sim 0.5$ . As to other mass ratios see the paper by Matsuda et al.,<sup>30)</sup> although they restricted their computational region to the vicinity of the primary star.

All physical quantities are normalized. The length is scaled by the separation  $A$ . With the rotational frequency of the binary being  $\Omega$ , the time is scaled as  $1/\Omega$ , so that the orbital period becomes  $2\pi$ . The density at the surface of the companion is taken to be 1. The gravity constant  $G$  is eliminated through the following equation.

$$A^3 \Omega^2 = G(M_1 + M_2). \quad (2.2)$$

A Cartesian coordinate system with the origin located at the center of the primary star is used. The x-axis is a line combining the centers of the primary and the companion. The center of the companion is at  $(-1, 0, 0)$ . The z-axis is perpendicular to the orbital plane and is oriented in the same direction as the angular momentum vector of orbital rotation. The  $x - y$  plane therefore constitutes the orbital plane.

The calculation region is a rectangular parallelepiped covering from  $(-1.5, -0.5, 0)$  to  $(0.5, 0.5, 0.5)$ . With the assumption of symmetry of physical quantities in relation to the orbital plane, the calculations are made only in the region of upper half. This region is divided with grid points of  $201 \times 101 \times 51$ .

## 2.2. Boundary Conditions and Initial Conditions

The primary star is assumed to be a hole occupying a region covering  $3 \times 3 \times 2$  and centered at the origin. The inside of the primary star is always filled with a gas having a density, sound speed and velocity of  $\rho_1$ ,  $c_1$  and 0, respectively. The pressure in the inside of the hole is kept sufficiently low in order to always absorb the surrounding gas. Here  $\rho_1$  and  $c_1$  are parameters. The mass accretion rate onto the main star is obtained by solving Riemann problem at each time step.

The companion is assumed to fill the critical Roche lobe. The inside of the companion is filled with a gas with density  $\rho_0 = 1$ , sound speed  $c_0$  and velocity 0, while the gravity is neglected in the companion. Here  $c_0$  is taken as a parameter and its effect is studied. The assumption that the gas inside the companion has 0 velocity does not mean that there is no gas outflow from the companion. The gas does flow out when the

Table I. Parameters.

Model	$c_0$	$\rho_1, c_1$	$\gamma$
A	0.02	$10^{-5}, \sqrt{10}$	1.01
B	0.02	$10^{-5}, \sqrt{10}$	1.2
C	0.02	$10^{-7}, 0.02$	1.01
D	0.02	$10^{-7}, 0.02$	1.2
E	0.1	$10^{-5}, \sqrt{10}$	1.01
F	0.1	$10^{-5}, \sqrt{10}$	1.2

pressure outside the companion is lower than that inside the companion. The outflow flux is calculated by solving Riemann problem at each time step.

The outside of the outer boundary is assumed to be always filled with a gas having a density  $\rho_1$ , sound speed  $c_1$  and velocity 0. Use of this boundary condition insures stable calculation. Here also inflow or outflow of the gas through the outer boundary is possible and the flux is calculated by solving Riemann problem between the inside and outside of the calculation region at each time step.

As the initial conditions, the whole region except the inside of the companion is occupied at time  $t = 0$  by the gas with density  $\rho_1$ , sound speed  $c_1$  and velocity 0. The initial density  $\rho_1$  and initial sound speed  $c_1$  are parameters, the effects of which are studied later. The model parameters used in the present work are summarized in the table 1.

Typically, calculations are continued up to an orbital period of more than 10. We confirm that the disk mass does not change appreciably after a few rotation period, so we may say that our computational results are nearly in steady state except insignificant oscillations.

### §3. Effect of Various Parameters on the Results of Calculations

#### 3.1. Effect of the Conditions of Gas Placed Initially in the Calculation Region

In our previous calculations,<sup>29-31)</sup> a gas with a density  $\rho_1 = 10^{-5}$  and a sound speed  $c_1 = \sqrt{10}$  was placed at time  $t = 0$ . This high sound speed means that the gas has a high temperature. This selection was made, since it was considered that such a high-temperature, low-density gas hardly falls onto the accretion disk or, if falls at all, affects the accretion disk only to a small extent.

The results obtained by the three-dimensional calculations, however, differed greatly, as described in Introduction, from those by the two-dimensional calculations. That is, the spiral arms with the three-dimensional calculations wind in more mildly than those with the two-dimensional calculations, even with the specific heat ratio  $\gamma = 1.01$ . This is attributable to the high temperature of the accretion disk obtained in the three-dimensional calculations, which in turn may be due to the high-temperature gas initially placed.

Unlike with two-dimensional calculations, the gas initially placed will, during progress of calculation and after an accretion disk has been formed, remain above the accretion disk. This initial gas may mix with the accretion disk, thereby increasing the temperature. We selected the density of the initial gas to be  $10^{-5}$ , which we considered to

be sufficiently small. However, the central part of the accretion disk, having a small thickness, may have been affected.

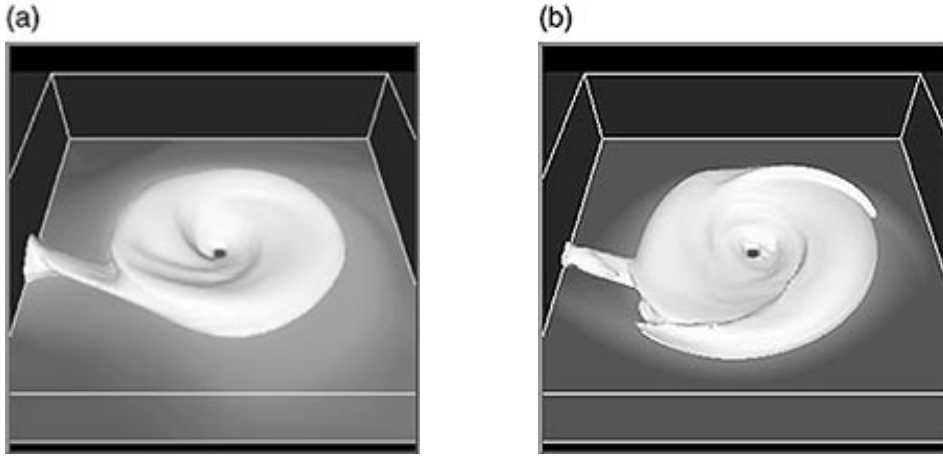


Fig. 3. Effect of the initially placed gas: Iso-density surfaces at  $\log \rho = -3.3$  of the disk for Model A with high temperature initial gas (a) and that at  $\log \rho = -4.0$  for Model C with low temperature and low density initial gas (b). The Model C shows clearer spiral shocks. In both cases, spiral shocks wind more loosely than that in two-dimensional calculations with  $\gamma = 1.01$ .

In the present study, we compare two cases with the initial gas having different densities and temperatures, in order to check their influence. Figure 3 shows the results. We may observe that Model C with low temperature and low density initial gas shows clearer and more openly wind spiral shocks than Model A with high temperature and high density initial gas. However, the difference may not be very significant, and in both cases, spiral shocks wind loosely even with  $\gamma = 1.01$ .

The key role is played, not by the temperature itself, but by the heat capacity, of the initial gas. A sufficiently low density of the initial gas therefore causes no problem with respect to heat capacity even when it has high temperature. Therefore, we may conclude that our previous choice of the initial condition is good enough, as far as the cases of  $\gamma = 1.01$  are concerned. The cases of  $\gamma = 1.2$  are slightly affected by the initial condition as will be discussed in 3.4.

### 3.2. Effect of the Surface Temperature of Companion

In our previous calculations, the gas placed at L1 point was assumed to have a sound speed of  $c_0 = 0.1$ . The present study includes the case of the gas present on the companion having a sound speed of  $c_0 = 0.1$ , which is, however, very large in actuality. If the binary has a typical speed of  $500 \text{ km s}^{-1}$ , the sound speed becomes  $50 \text{ km s}^{-1}$ , corresponding to a temperature of as high as  $2.5 \times 10^5 \text{ K}$ .

This high sound speed has been selected, because a high temperature on the surface of the companion increases the rate of the gas flowing out through the L1 point, so that calculation can proceed fast. Since, however, the above high temperature is unrealistic, the present study also includes the case of  $c_0 = 0.02$  corresponding to  $10^4 \text{ K}$ .

Figure 4 shows, with  $\gamma = 1.01$ , the influence of the surface temperature of the companion. With the high temperature, the L1 stream becomes thick and its inflow rate increases. On the other hand, with the low temperature, which may be more



realistic, the L1 stream becomes thin. Model E shows clearer and more widely open spiral shocks than Model A, because of larger disk size.

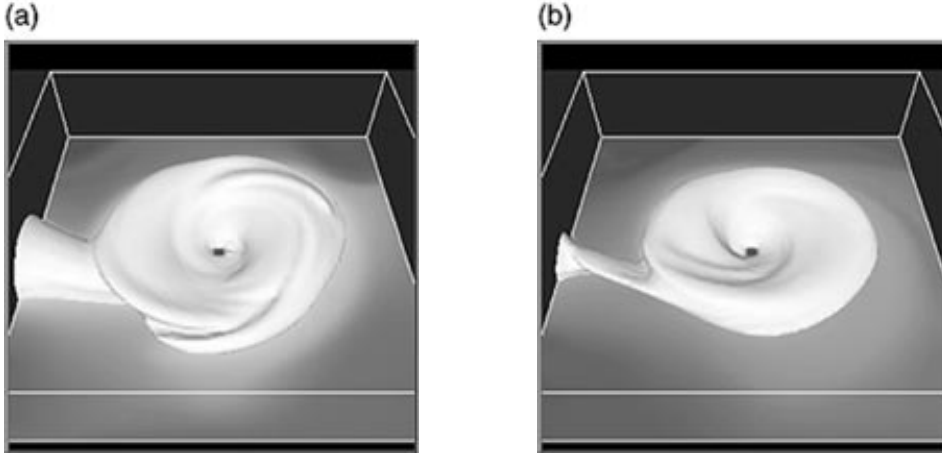


Fig. 4. Effect of the surface temperature of companion: Iso-density surfaces at  $\log \rho = -2.5$  for Model A with high surface temperature of companion (a), and that at  $\log \rho = -3.3$  for Model E with low surface temperature (b). With the high surface temperature of companion, the L1 stream becomes thick and the inflow rate high and the disk becomes large. In Model E, spiral shocks become clearer and wind more loosely than that in Model A.

### 3.3. Effect of Specific Heat Ratio

As commented in Introduction, the influence of radiative cooling is very important in accretion disks. Without this cooling, the temperature of an accretion disk would become the virial temperature, which is very high. It is however not practical to perform any three-dimensional simulation of radiative fluid dynamics accurately with computing capability currently available.

Therefore, workers in this field have been used either an equation of state with low specific heat ratio like us, that of iso-thermal gas or that of iso-entropy gas. A low specific heat ratio is selected in the present work in order to emulate the influence of radiative cooling. Although the ionized plasma gas present in actual accretion disks has a specific heat ratio of  $5/3$ , the present calculations use  $\gamma = 1.01, 1.2$ . Our calculations thus, in a strict sense, simulate a poly-atomic molecular gas. In this case, when the gas is compressed, its energy, being distributed to the degree of internal freedom, will not contribute to translational motion to a large extent, so that the temperature elevation is suppressed. This internal energy is convected with gas and eventually accreted by the central object, and is not radiated away to the outer space. Nevertheless the low ratio of specific heats emulates radiative cooling somehow. The calculation including the radiative transfer is now work in progress (Nagae et al. 2001).

In the limit of  $\gamma = 1$ , the gas becomes isothermal. The equation of state adopted by us, however, does not allow  $\gamma = 1$ . We therefore select  $\gamma = 1.01$ , which is the minimum value in view of calculation accuracy. As a counterpart, we select  $\gamma = 1.2$ , above which experience tells us no accretion disk can ever form. Figure 5 shows the results.

With  $\gamma = 1.01$ , a clear accretion disk and shock waves appear under all the initial conditions or boundary conditions assumed. On the other hand, with  $\gamma = 1.2$ , the

shape of the accretion disk finally obtained varies depending on the initial conditions and boundary conditions. In Model B and F the accretion disks are highly distorted, while in Model D we may observe a normal accretion disk. In all cases, the temperature of the disk is more higher than that of the disk in its outburst.

Bisikalo et al.<sup>32)</sup>rf:36 argue that no accretion disk forms with  $\gamma = 1.2$ , which is not completely inconsistent with our results. At any rate, it is expected that a specific heat ratio larger than 1.2 may produce no accretion disk under any initial or boundary conditions.

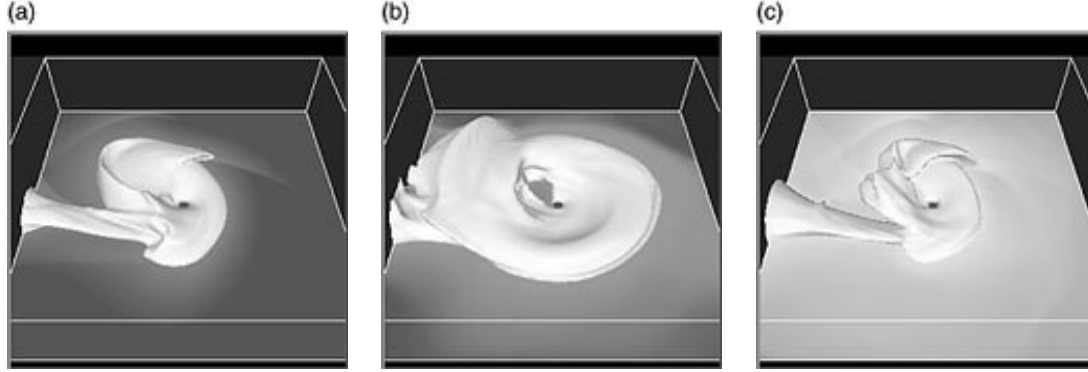


Fig. 5. Iso-density surfaces for a specific heat ratio of  $\gamma = 1.2$ , under different boundary conditions and initial conditions: (a) Model B at  $\log \rho = -3.7$ . (b) Model D at  $\log \rho = -4.0$ , with low density and low temperature of initial gas. (c) Model F at  $\log \rho = -2.9$ , with high temperature at the surface of the companion. With  $\gamma = 1.2$ , disk is affected significantly by both initial and boundary conditions.

#### §4. Detailed Structure of Flow

##### 4.1. Penetration of the L1 Stream into the Accretion Disk and Formation of an L1 Shock

In order to investigate the detailed structure of the accretion disk and the L1 stream, let us investigate the details of some specific models in this section. Since the case of specific heat ratio  $\gamma = 1.2$  corresponds to too high a temperature of the disk, only the case  $\gamma = 1.01$  is studied here. In the present case,  $c_0 = 0.02$  is taken as the sound speed on the surface of the companion.

Figure 6 shows the iso-density surfaces at various levels of Model C. And figure 7 shows the iso-density surface of the same model from a different view angle. One may observe cross-sectional structures of a spiral shock and the L1 shock. The spiral shock seems to be concave to the upstream, while the L1 shock is convex. One may conclude that the L1 shock is a bow shock.

The figures so far presented show only iso-density surfaces, which cannot reveal any detailed structure, in particular the velocity distribution, of the flow. Hereafter let us investigate the interaction between the L1 stream and the accretion disk, with use of the velocity distribution.

Figure 8 shows velocity distributions on x-y planes at various heights by means of the Line Integration Convolution (LIC) method. The figure shows that on the orbital

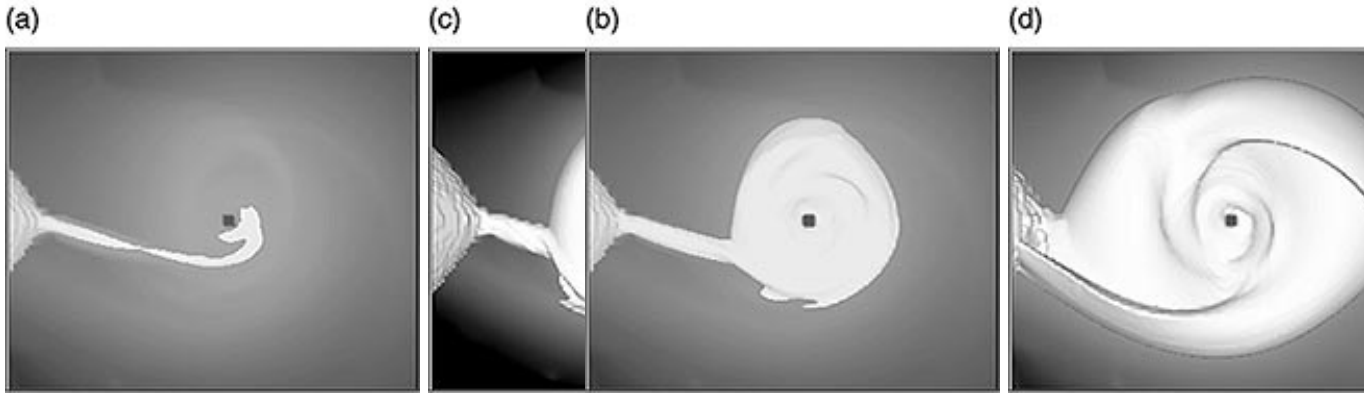


Fig. 6. Iso-density surfaces for Model C at various density levels: (a)  $\log \rho = -2.0$ . (b)  $\log \rho = -3.0$ . (c)  $\log \rho = -4.0$ . (d)  $\log \rho = -5.0$ .

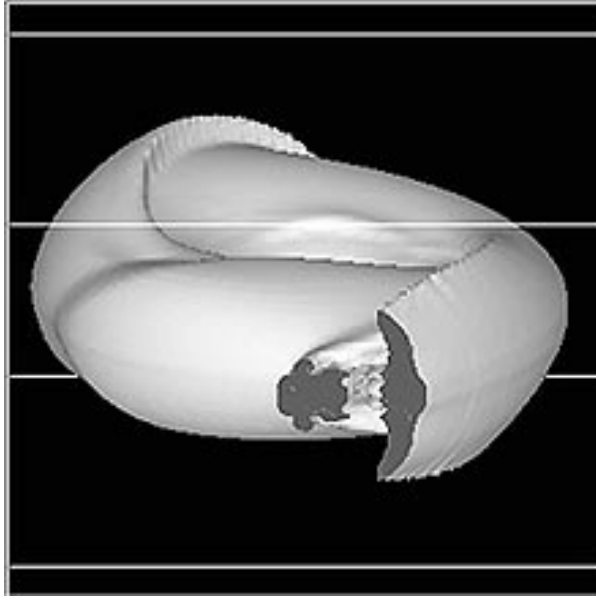


Fig. 7. The same as figure 6 at  $\log \rho = -4.0$  but seen from a different angle. One may observe cross sections of a spiral shock and the L1 shock. The spiral shock is concave to the upstream, while the L1 shock is convex to the upstream. This means the L1 stream is a bow shock.

plane of  $z = 0$ , gas in the accretion disk collides with the L1 stream and, as a result, loses its angular momentum and falls towards the primary star. A bow shock is then formed close to and parallel with the high-density, spear-like L1 stream (above the L1 stream in the figure). On  $z = 0.08$ , the gas of the accretion disk rotates about the central star. The influence of the L1 stream is thus limited to a region near the orbital plane.

Figure 9 presents, in order to observe the above phenomena more closely, flow patterns, drawn by means of the LIC method, on the iso-density surface. The figure shows the internal structure more clearly with increasing density of the iso-density surface. Figure 10 shows a three-dimensional view of the streamlines.

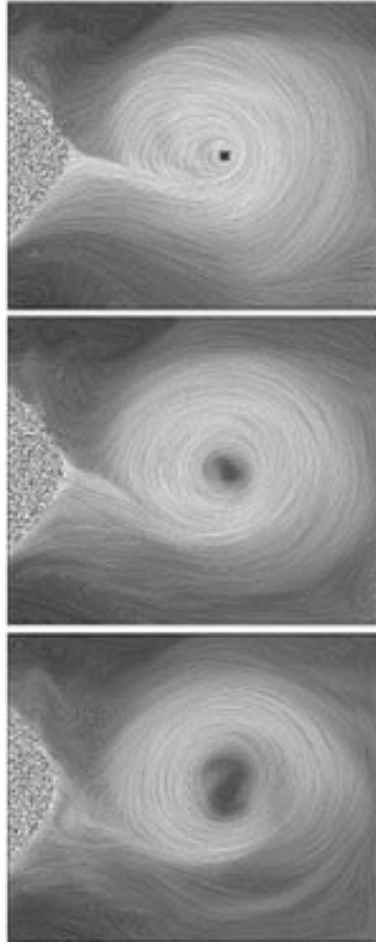


Fig. 8. Flow patterns on the orbital plane and on x-y planes at various heights, for Model A, are shown by means of the LIC method. The degree of whiteness represents the magnitude of density. From top to bottom  $z = 0$ ,  $z = 0.04$ ; and  $z = 0.08$ . On the orbital plane with  $z = 0$ , the gas in the accretion disk collides with the L1 stream and, as a result, loses its angular momentum and falls towards the central star. On  $z = 0.08$ , the gas of the accretion disk rotates about the central star. The influence of the L1 stream is thus limited to a region near the orbital plane.

These pictures are particularly interesting, because they show two remarkable features. 1) The L1 stream penetrates into the accretion disk. 2) The disk gas having collided with the L1 stream abruptly changes, due to the L1 bow shock formed, its direction towards the primary star.

#### 4.2. Influence of the L1 Stream on the Disk Gas

Figure 11 shows, in order to study the influence of the L1 stream on the disk gas, the distribution of the entropy related function of the gas  $S = p/\rho^\gamma$  obtained by two-dimensional and three-dimensional calculations, with the abscissa representing the distance from the central star and the ordinate the entropy:  $\log(S)$ . Dispersion in the plots in the ordinate direction corresponds to that in the values at various angular positions.

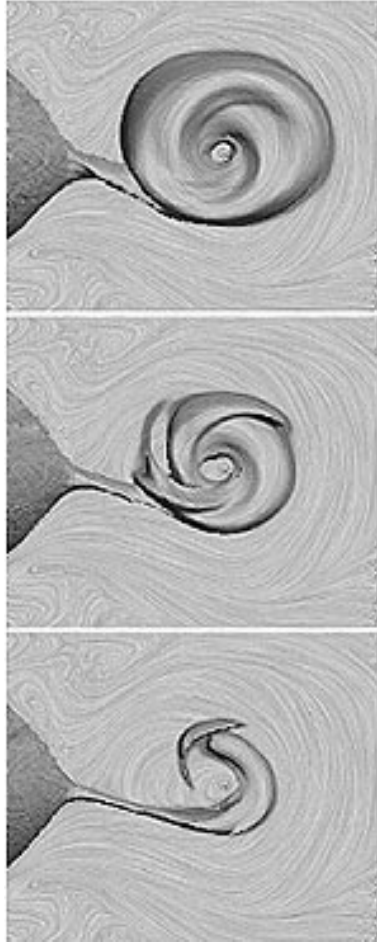


Fig. 9. Iso-density surfaces and flow patterns thereon, together with a flow pattern on the orbital plane, of Model A drawn by LIC method. From top to bottom at  $\log \rho = -3.3, -3.0, -2.7$  all at time  $t = 75.36$ .

We discuss, in particular, the case of  $\gamma = 1.01$ , where,  $S$  being almost the same as temperature, the figure can be considered to be showing the temperature distribution. The figure clearly shows a smaller dispersion with two-dimensional calculations than with three-dimensional calculations. This means that the entropy and temperature distributions in two-dimensional cases are nearly axisymmetric, which in turn means that the entropy increases due to spiral shocks, only to a moderate extent. The entropy values in the central zone (the left end) and the peripheral zone (the right end) are lower with two-dimensional calculations than with three-dimensional ones. A large dispersion in the values with three-dimensional calculations is caused by the L1 shock generated on collision between the L1 stream and the disk gas. In particular, a horizontal linear distribution of  $S$ , seen in a region corresponding to large radii, is due to the L1 shock. Accordingly, with three-dimensional calculations, a high entropy or high temperature of the gas decreases the Mach number of the gas, so that spiral shocks wind in mildly even with  $\gamma = 1.01$ .

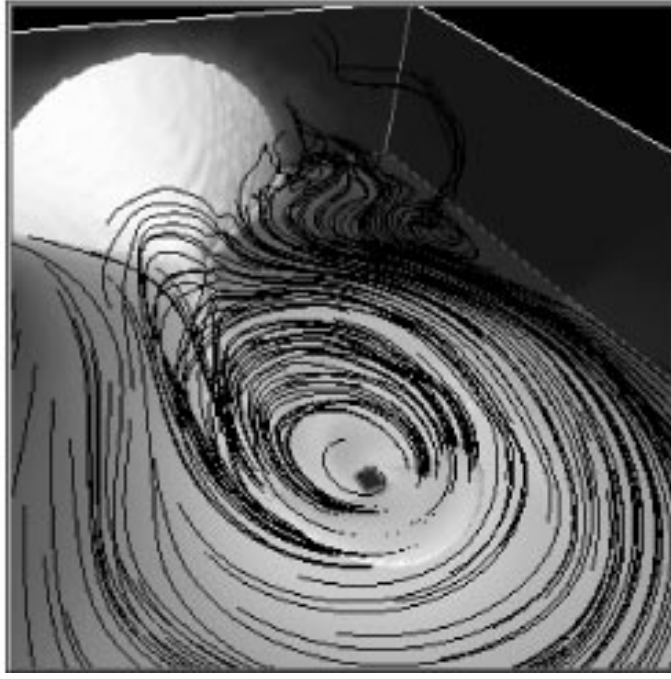


Fig. 10. Three-dimensional view of streamlines of model A.

Figure 11 also shows the entropy distribution for the case of  $\gamma = 1.2$ . In this case, although the distribution is wider in three-dimensional calculations than two-dimensional ones, the absolute values are almost the same in both calculations. The angle of winding-in of spiral shocks is therefore almost the same with both two-dimensional and three-dimensional calculations.

#### 4.3. *Effective $\alpha$*

The accretion disk has a large non-axisymmetry in its density distribution because of the loosely wound spiral shocks in our calculations. In the spiral shock model of angular momentum transfer, tidal torque from the secondary star transfers the angular momentum of gas in the accretion disk to the angular momentum of the orbital motion of the binary system. Angular momentum transfer becomes more effective as spiral shocks wind more loosely and, as a result, the non-axisymmetry of density distribution becomes large.

In our calculations, the disk gas loses its angular momentum not only through spiral shocks, but on interaction with the penetrating L1 stream.

The disk gas loses its angular momentum on collision with the penetrating L1 stream. In this process, angular momentum is transferred directly from the disk gas to the penetrating L1 stream. This angular momentum transfer is extremely effective on the equatorial plane. In figure 8, the streamlines of the disk gas is bent on collision with the penetrating L1 stream. This mechanism is effective, but is closed in the disk. The angular momentum transferred to the penetrating L1 stream is finally released into the central part of the disk. This mechanism is, therefore, angular momentum re-distribution rather than angular momentum transfer.

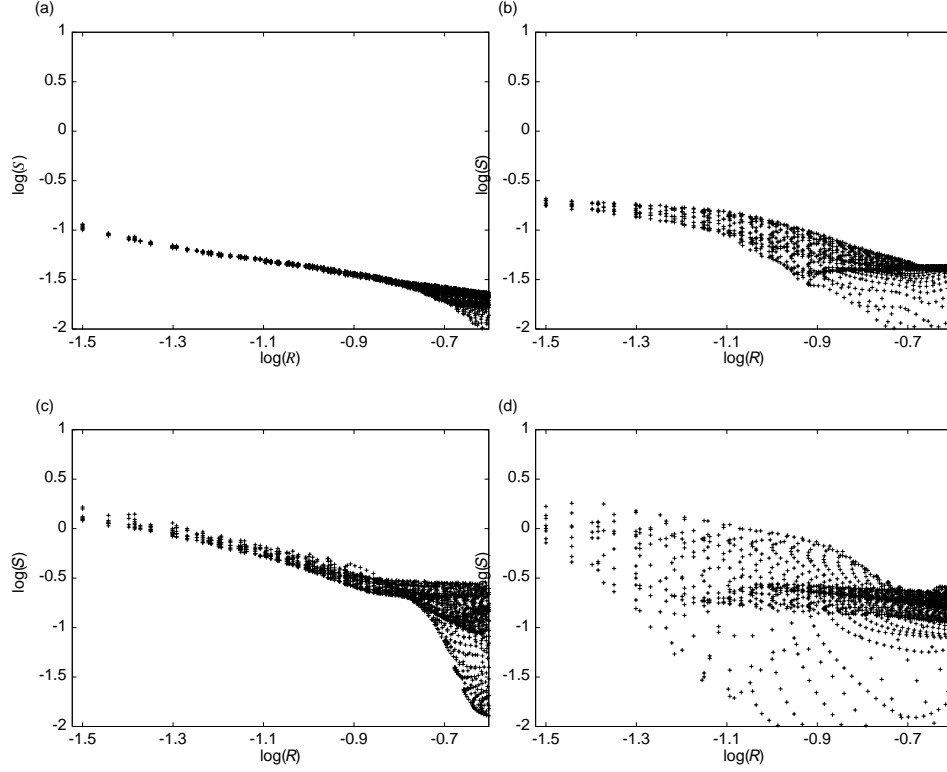


Fig. 11. Radial distribution of entropy  $\log(p/\rho^\gamma)$  in the accretion disk. The top row corresponds to  $\gamma = 1.01$ , and the bottom row to  $\gamma = 1.2$ . The left-side column shows the case with two-dimensional calculations and the right-side column that with three-dimensional calculations. Other parameters are  $\rho_1 = 10^{-7}$ ,  $c_1 = 0.02$ , and  $c_0 = 0.02$ . In three-dimensional calculations, entropy increases rapidly at the peripheral zone due to the L1 shock. This increase of entropy is significant with  $\gamma = 1.01$ .

The L1 shock produced on collision between the disk gas and the penetrating L1 stream contributes to a non-axisymmetry in density distribution in the disk, and the disk gas loses its angular momentum through the L1 shock. These two mechanisms are effective in the peripheral part of the disk into which the L1 stream is penetrating.

We calculate the effective  $\alpha$ , according to Frank, King & Raine,<sup>41)</sup>

$$\nu = \frac{\dot{M}}{3\pi\Sigma} \left[ 1 - \left( \frac{R_*}{R} \right)^{\frac{1}{2}} \right], \quad (4.3)$$

$$\alpha = \frac{\nu}{c_s H}, \quad (4.4)$$

where  $\nu$  is kinematic viscosity,  $\dot{M}$  is mass accretion rate,  $\Sigma$  is surface density,  $R_*$  is radius of the primary star,  $R$  is distance from the primary star,  $c_s$  is sound speed and  $H$  is scale height. We neglect  $\left(R_*/R\right)^{\frac{1}{2}}$  because  $R_*/R \ll 1$ . Figure 12 shows the effective  $\alpha$  at each orbital period for Model A. The effective  $\alpha$  varies with both of radius and time, its maximum being  $\alpha \sim 0.3$ .

In Spruit<sup>15)</sup> and Livio & Spruit,<sup>42)</sup> the effective  $\alpha$  depends on the mass ratio and the pitch angle of spiral shock. However, the analytical value of the effective  $\alpha$  is of order of  $\sim 10^{-2}$ , while in two-dimensional calculations by Matsuda et al.<sup>11)</sup>, the effective  $\alpha$  is of the order 0.1 with large  $\gamma$ .

The effective  $\alpha$  is large in the peripheral part. In this region, the non-axisymmetric density distribution is enhanced by the L1 shock, and therefore, the disk gas loses effectively its angular momentum due to tidal torque from the secondary star. The disk gas also loses its angular momentum on collision with the penetrating L1 stream in the peripheral part. On the other hand, in the central part, the effective  $\alpha$  is of the order 0.1, and this value is similar to that in two dimensional calculations with large  $\gamma$  and loosely wound spiral shocks.

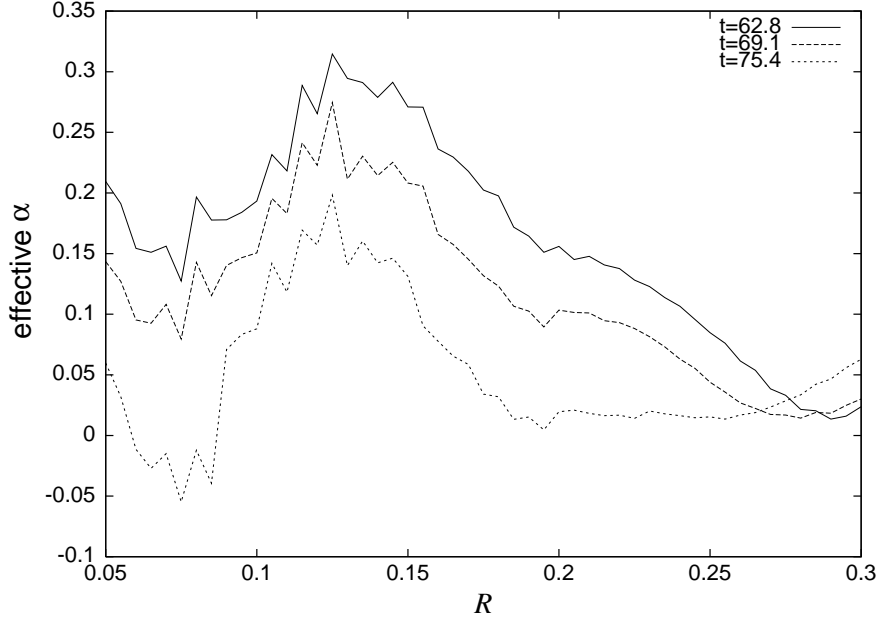


Fig. 12. Radial distributions of effective  $\alpha$  averaged in azimuthal direction at 10, 11 and 12 orbital periods for Model A. Effective  $\alpha$  oscillates in time, but its peak is located at  $R \sim 1.2$  and the value decreases with radius. The maximum value of effective  $\alpha$  is  $\sim 0.3$ .

#### 4.4. Formation of the 'hot spot'

In our three-dimensional simulation, the effect of radiative cooling is neglected, and therefore the accretion disk becomes hot. This hot disk becomes thick and of low density, so that the dense L1 stream can penetrate into the disk and the 'hot line' is formed along the penetrating L1 stream.

On the other hand, in two-dimensional simulations, the disk cannot expand along the  $z$ -axis, and therefore the density of the disk becomes larger than that of the L1 stream. And the L1 stream collides with the disk edge and does not penetrate into the disk.<sup>6)</sup> rf:14 Rozyczka & Schwarzenberg-Czerny<sup>43)</sup> and Rozyczka<sup>44)</sup> performed two-dimensional simulations of the collision between the L1 stream and the disk edge. They showed that the collision between the L1 stream and the disk edge forms two shock



waves and concluded that these shock waves are considered as the 'hot spot'.

The difference of the density between the disk and the L1 stream is important. Whether or not the L1 stream penetrates into the disk depends on the magnitude of each of the densities. If the density of the disk is larger than that of the L1 stream in the three-dimensional simulation, the L1 stream will be stopped on collision with the disk edge and the hot spot will be formed.

In order to investigate collision between the L1 stream and the dense accretion disk, we suddenly changed the density of the surface of the secondary star from 1 to 0.5, after the accretion disk has reached steady state. In this case, the density of the L1 stream decreases and becomes of the same order of magnitude with the density at the disk edge. Figure 13 shows the density contours on the equatorial plane in the vicinity of the collision point. The L1 stream is stopped on collision with the disk edge, and shock waves are formed at the collision point. These features are similar to the results of two-dimensional simulations.

If the effect of radiative cooling is considered, the accretion disk will become cool, thin and of high density. In such conditions, we consider that the L1 stream cannot penetrate into the dense disk and that the 'hot spot' is formed on collision between the L1 stream and the disk.

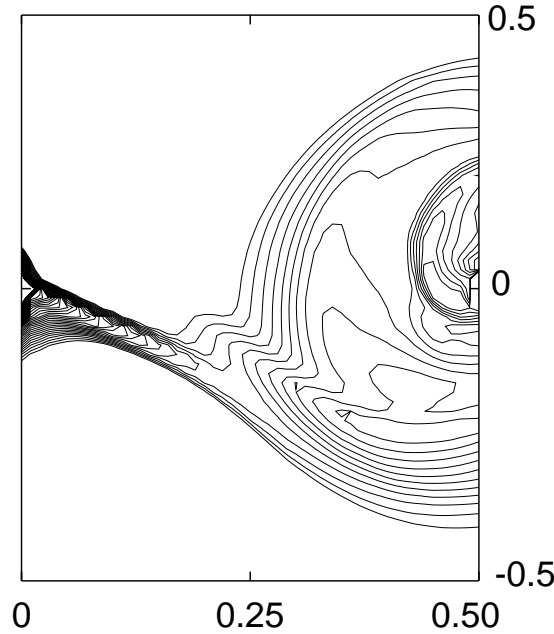


Fig. 13. Density contours on the equatorial plane. The density of the L1 stream at the collision point is of the same order of magnitude with the density of the disk edge. The L1 stream is stopped on collision with the disk edge and shock waves are formed. These features are similar to the results of two-dimensional simulations.

#### 4.5. *Flows on the Companion*

We have so far paid attention to the accretion disk and the L1 stream. Since our calculation region includes the companion, it is also of interest how the flows on the surface of the companion behave, although we may not recognize this with observational means currently available.

The coordinate system we employed is Cartesian, which can hardly represent precisely the companion having a nearly spherical surface. Outer boundaries may also affect the surface flow of the companion. We have to examine the results with these restrictions in mind. Figure 14 shows flows on the surface of the companion for case A at 9 orbital periods. Figures are produced using Pixel Exposure Method (PEM). Worth noticing is that flows towards the L1 point start even at high-latitude regions. This main flow pattern is almost steady, although small flow patterns change.

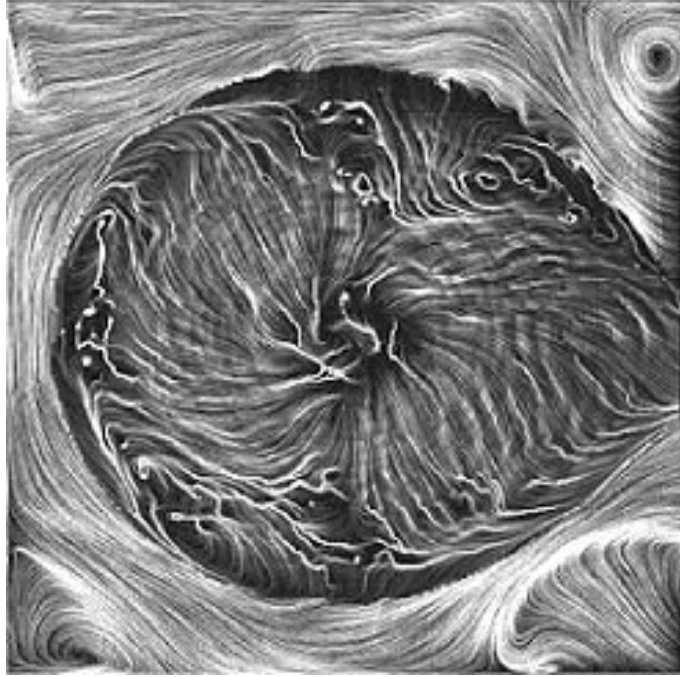


Fig. 14. Flows on the surface of companion produced by Pixel Exposure Method for case A at  $t = 56.52$ . The value of density on which the flows are plotted is  $\log \rho = -3.5$ . Gas which outflows from high-latitude regions flows toward the L1 point. This main flow pattern is almost steady, although small flow patterns change. Much attention should not be paid on vortices at the corner of the rotational plane, because they may be affected by the outer boundary condition.

It is also interesting to note that eddy patterns have been formed on the surface of the companion. This is considered to be similar to vortices of low pressure or high pressure generating on the surface of Earth or Jupiter. It is expected that flows on the surface of the companion in a binary system do not form any simple regular pattern but become complex flows. However, the above restrictions allow no definite conclusions to be drawn. Calculations with generalized curvilinear coordinates fitting the shape of the companion surface are desired.

## §5. Conclusions and Discussion

### 5.1. Conclusions

We performed numerical simulations for an ideal gas constituting an accretion disk in a close binary with mass ratio 1, with a specific heat ratio of  $\gamma = 1.01, 1.2$  and compared two-dimensional with three-dimensional calculations. From the results obtained, we conclude as follows.

1. Whether or not the calculation region may include the companion, no significant difference appears in the results.
2. An initial condition for gas to be placed at  $t = 0$  of  $\gamma = 1.01$  does not have a large influence, while that of  $\gamma = 1.2$  has.
3. A high temperature of gas present on the surface of the companion gives a thick L1 stream, while a low temperature a fine one; both do not have very much influence on the structure of the accretion disk.
4. A specific heat ratio of  $\gamma = 1.01$  gives, for any parameter, a neat-shaped accretion disk with spiral shocks. On the other hand, with  $\gamma = 1.2$  the accretion disk formed sometimes takes a greatly distorted shape depending on the values of parameters.
5. The L1 stream does not reduce its velocity on collision with the accretion disk or form a hot spot, but forms a bow shock, which can be called an L1 shock, or a hot line rather than a hot spot.
6. The L1 shock and the penetrating L1 stream enhance the non-axisymmetry in density distribution in the disk, so that angular momentum transfer by tidal torque from the secondary star becomes more effective.
7. Complex vortices may be present on the surface of the companion.

### 5.2. Discussion

#### 5.2.1. Bisikalo *et al.*'s work

Attention should be paid here to a series of calculations made by Bisikalo *et al.* <sup>32)rf:36</sup> They performed, like ourselves, numerical simulations of accretion disks by means of the finite difference method. Our calculation scheme differs from theirs in that we use a far larger number of cells, thus achieving a higher calculation accuracy, although our calculation region is a little narrower than theirs. Nevertheless, their results, varying to some extent though, are basically similar to ours. In particular, their results, like ours, show no hot spots. They further argue that the luminosity curve of a close binary can be explained even in the absence of hot spots.

We also differ from them in the way to explain the mechanism involved in generation of shocks. We contend, as before, that spiral shocks are formed due to the tidal force exerted by the companion, and that the L1 shock occurs on collision between the L1 stream and the disk flow. On the other hand, they do not admit the effect of the tidal force and, further, propose a mechanism of the shock formation as caused by collision between the disk flow and the envelope. The fact that our results are similar to theirs is still worth noticing, although the interpretations are somewhat different, and desired to be checked by a third party.

### 5.2.2. *Bath et al.'s work*

Bath, Edwards & Mantle<sup>45)</sup> have discussed the penetration of the L1 stream into the accretion disk. According to their discussion, whether or not the L1 stream penetrates into the accretion disk depends on the magnitude of each of the densities. That is, an L1 stream having a density larger than that of the accretion disk penetrates into the accretion disk. Our calculations just correspond to this case; the density of our L1 stream is as high as about 10 times that of the accretion disk. On the other hand, an L1 stream having a low density will form a hot spot on collision with the accretion disk. This case probably corresponds to the quiescent phase having a hot spot. In this case the disk temperature is lower than that in the outburst phase due to the lack of the L1 shock, and the spiral shocks wind more tightly and they may not be observable by the Doppler tomography technique.

Bath et al.<sup>45)</sup> call the L1 shock, or the hot line we refer to in the present paper, which we have found by means of calculations, a shock-heated wall. With respect to observation of an actual penetration, Chochol et al.<sup>46)</sup> argue that it is observable in the symbiotic star CI Cyg, and Skidmore et al.<sup>47)</sup> also argue in the dwarf nova WZ Sge.

The magnitude of the density of an L1 stream depends on the surface temperature of the companion. With a low surface temperature, the L1 stream becomes thin and of low density, so that it may not penetrate into the accretion disk.

## Acknowledgements

The authors thank Mr. E. Hayashi for his contribution to preparing a draft of this paper. T. Matsuda is supported by Grant-in-Aid for Scientific Research of Ministry of Education, Science and Culture in Japan (11134206) and (10640231) of JSPS. Our calculations were mainly carried out on NEC SX-4 at the Data Processing Center of Kobe University and partly on Fujitsu VPP300/16R, VX/4R at the Astronomical Data Analysis Center of the National Astronomical Observatory, Japan.

## References

- 1) D. Steeghs, E. T. Harlaftis and K. Horne, *Mon. Not. R. Astron. Soc.* **290** (1997), L28.
- 2) D. Steeghs, K. Horne, T. R. Marsh and J. F. Donati, *Mon. Not. R. Astron. Soc.* **281** (1996), 626.
- 3) M. D. Still, D. A. H. Buckley and M. A. Garlick, *Mon. Not. R. Astron. Soc.* **299** (1998), 545.
- 4) V. Joergens, H. C. Spruit and R. G. M. Rutten, *Astro. Astrophys.* **356** (2000), L33.
- 5) V. V. Neustroev and N. V. Borisov, *Astro. Astrophys.* **336** (1998), L73.
- 6) K. Sawada, T. Matsuda and I. Hachisu, *Mon. Not. R. Astron. Soc.* **219** (1986), 75.
- 7) K. Sawada, T. Matsuda and I. Hachisu, *Mon. Not. R. Astron. Soc.* **221** (1986), 679.
- 8) K. Sawada, T. Matsuda, M. Inoue and I. Hachisu, *Mon. Not. R. Astron. Soc.* **224** (1987), 307.
- 9) H. C. Spruit, T. Matsuda, M. Inoue and K. Sawada, *Mon. Not. R. Astron. Soc.* **229** (1987),

517.

- 10) M. Rozyczka and H. C. Spruit, in *Theory of Accretion Disks*, ed F. Meyer, W. J. Duschl, J. Frank and E. Meyer-Hefmeister (Kluwer, Dordrecht, 1989) p341.
- 11) T. Matsuda, N. Sekino, E. Shima, K. Sawada and Spruit H, *Astro. Astrophys.* **235** (1990), 211.
- 12) M. Rozyczka and H. C. Spruit, *Astrophys. J.* **417** (1993), 677.
- 13) G. J. Savonije, J. C. B. Papaloizou and D. N. C. Lin, *Mon. Not. R. Astron. Soc.* **268** (1994), 13.
- 14) P. Godon, 1997, *Astrophys. J.* bf 480 (1997), 329.
- 15) H. C. Spruit, *Astro. Astrophys.* **184** (1987), 173.
- 16) D. Molteni, G. Belvedere and G. Lanzafame, *Mon. Not. R. Astron. Soc.* **249** (1991), 748.
- 17) M. Hirose, Y. Osaki and S. Mineshige, *PASJ.* **43** (1991), 809.
- 18) M. Nagasawa, T. Matsuda and Kuwahara K, *Numer. Astroph. in Japan* **2** (1991), 27.
- 19) G. Lanzafame, G. Belvedere and D. Molteni, *Mon. Not. R. Astron. Soc.* **258** (1992), 152.
- 20) G. Lanzafame, G. Belvedere and D. Molteni, *Mon. Not. R. Astron. Soc.* **263** (1993), 839.
- 21) Z. Meglicki, D. Wickramasinghe and V. Bicknel, *Mon. Not. R. Astron. Soc.* **264** (1993), 691.
- 22) R. Whitehirst, *Mon. Not. R. Astron. Soc.* **266** (1994), 35.
- 23) J. C. Simpson, *Astrophys. J.* bf 448 (1995), 822.
- 24) H. Yukawa, H. M. J. Boffin, T. Matsuda, *Mon. Not. R. Astron. Soc.* **292** (1997), 321.
- 25) G. Lanzafame and G. Belvedere, *Mon. Not. R. Astron. Soc.* **284** (1997), 957.
- 26) G. Lanzafame and G. Belvedere, *Mon. Not. R. Astron. Soc.* **295** (1998), 618.
- 27) H. M. J. Boffin, K. Haraguchi and T. Matsuda T, in *Proceedings of the international conference on "Disk Instabilities in Close Binary Systems — 25 Years of the Disk-Instability Model"*, ed S. Mineshige and J. C. Wheeler (Universal Academy Press, Tokyo, 1999) p147 .
- 28) K. Sawada and T. Matsuda, *Mon. Not. R. Astron. Soc.* **255** (1992), s17.
- 29) M. Makita and T. Matsuda, in *Numerical Astrophysics*, ed S. M. Miyama, K. Tomisaka and T. Hanawa (Kluwer, Boston, 1999) p227.
- 30) T. Matsuda, M. Makita and H. M. J Boffin, in *Proceedings of the international conference on "Disk Instabilities in Close Binary Systems — 25 Years of the Disk-Instability Model"*, ed S. Mineshige and J.C Wheeler (Universal Academy Press, Tokyo, 1999) p129.
- 31) M. Makita, K. Miyawaki and T. Matsuda, *Mon. Not. R. Astron. Soc.* **319** (2000), 906.
- 32) D. V. Bisikalo, A. A. Boyarchuk, O. A. Kuznetsov and V. M. Chechetkin, *Astron. Reports* **41** (1997), 786.

- 33) D. V. Bisikalo, A. A. Boyarchuk, O. A. Kuznetsov, V. M. Chechetkin, *Astron. Reports* **41** (1997), 794.
- 34) D. V. Bisikalo, A. A. Boyarchuk, V. M. Chechetkin, O. A. Kuznetsov, and D. Molteni, *Mon. Not. R. Astron. Soc.* **300** (1998), 39.
- 35) D. V. Bisikalo, A. A. Boyarchuk, O. A. Kuznetsov and V. M. Chechetkin, *Astron. Reports* **42** (1998), 33.
- 36) D. V. Bisikalo, A. A. Boyarchuk, O. A. Kuznetsov and V. M. Chechetkin, *Astron. Reports* **42** (1998), 621.
- 37) T. Matsuda, M. Makita, H. Fujiwara, T. Nagae, K. Haraguchi, E. Hayashi, and H. M. J. Boffin, *Ap&SS* **274** (2000), 259.
- 38) T. Matsuda, N. Tamura and K. Sawada, *J. Fluid Mech.* **201** (1989), 203.
- 39) T. Jyounouchi, I. Kitagawa, S. Sakashita and M. Yasuhara, *Proc. 7th CFD Symp.* (1993).
- 40) E. Shima and T. Jyounouchi, *NAL-SP27, Proceedings of 12th NAL symposium on Aircraft Computational Aerodynamics* (1994), p255.
- 41) J. Frank, A. King and D. Raine, *Accretion Power in Astrophysics* (Cambridge University Press, Cambridge, 1992)
- 42) M. Livio and H. Spruit, *A&A* **252** (1991), 189
- 43) M. Rozyczka and A. Schwarzenberg-Czerny, *AcA* **37** (1987), 141
- 44) M. Rozyczka, *AcA* **38** (1988), 175
- 45) G. T. Bath, A. C. Edwards and V. J. Mantle, *Mon. Not. R. Astron. Soc.* **205** (1983), 171.
- 46) D. Chochol, A. Vittone, L. Milano and L. Rusconi, *Astro. Astrophys.* **140** (1984), 91.
- 47) W. Skidmore, E. Mason, S. B. Howell, D. R. Ciardi, S. Littlefair and V. S. Dhillon, *Mon. Not. R. Astron. Soc.* **318** (2000), 429.